A multi-organ integrated QSP model for hematopoietic stem cell differentiation to predict the immune cell reconstitution in ex-vivo gene therapy

Yuezhe Li[1], Eric Jordie[1], Tim Knab[1]
[1]*Metrum Research Group, Tariffville, CT, USA*

Abstract

The differentiation of mammalian hematopoietic stem cells (HSCs) is complex and multi-scale, providing an opportunity for mathematical modeling and simulation to aid in mechanistic understanding, and ultimately, to inform drug development efforts. Historically, HSC mathematical models were focused on the development of a subset of cells, but mathematical models encompassing the overall cellular system's complexity are rarely available. Here, an integrated quantitative systems pharmacology (QSP) model that characterizes multi-organ HSC differentiation was developed by integrating literature models and adding novel features. The result is a more comprehensive representation of mammalian HSC development. This integrated model captured the reconstitution of red blood cells (RBCs), B cells, and T cells following HSC transplant in mice, and predicted the reconstitution of granulocytes and lymphocytes in patients with adenosine deaminase-deficient severe combined immunodeficiency (ADA-SCID) who underwent ex-vivo gene therapy.

Methods

The integrated models depicted HSC differentiation into erythrocytes, lymphocytes, and granulocytes were built sequentially by incorporating novel physiological-based features based on literature models and data in four sequential steps:

- Implemented an existing human HSC -> RBC differentiation model in [1]
- Scaled the HSC -> RBC differentiation model from human to mouse based on mouse physiology
- Integrated thymic T cells development model from [3], B cells development model from [2], and HSC -> granulocyte differentiation model into the mouse HSC differentiation model.
- Scaled the integrated mouse HSC differentiation model to human based on human physiology

Parameter tuning was carried out to help harmonize the difference across models. The integrated models for mouse and human were validated using cell reconstitution in peripheral blood after stem cell transplant/ ex-vivo gene therapy.

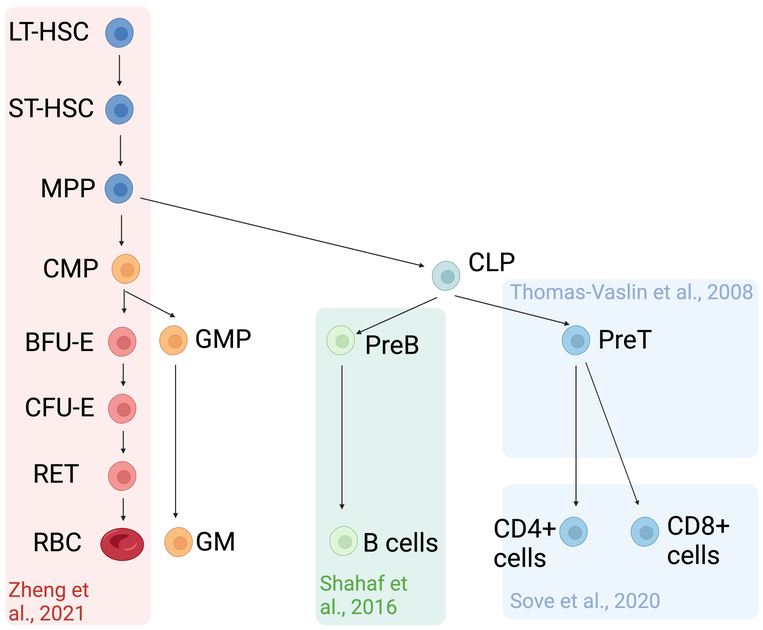

Fig 1. Summary diagram of this integrated model.

References

[1] Zheng, Bo, et al. CPT: Pharmacometrics & Systems Pharmacology 10.7 (2021): 696-708.
[2] Shahaf, Gitit, et al. Frontiers in immunology 7 (2016): 77.
[3] Thomas-Vaslin, Veronique, et al. The Journal of Immunology 180.4 (2008): 2240-2250.
[4] Sové, Richard J., et al. CPT: pharmacometrics & systems pharmacology 9.9 (2020): 484-497.
[5] Busch, Katrin, et al. Nature 518.7540 (2015): 542-546.
[6] Famili, Farbod, Anna-Sophia Wiekmeijer, and Frank JT Staal. Future science OA 3.3 (2017): FSO186.
[7] Spits, Hergen. Current opinion in immunology 6.2 (1994): 212-221.
[8] Whitmore, Kathryn V., and Hubert B. Gaspar. Frontiers in immunology 7 (2016): 314.
[9] Ribeil, Jean-Antoine, et al. New England Journal of Medicine 376.9 (2017): 848-855.
[10] Aiuti, Alessandro, et al. New England Journal of Medicine 360.5 (2009): 447-458.

Source Code

https://github.com/metrumresearchgroup/2023-ACoP-14-gene-therapy

Conclusion

Through integrating existing models and adding novel features, we developed mathematical models that provide a more comprehensive representation of mammalian HSC development. These integrated models were based on physiological understanding of mouse and human, and were validated accordingly. The models successfully predicted cell reconstitution after ex-vivo gene therapy and HSC transplant. These models provide a versatile platform for further development to inform drug development for ex-vivo gene therapy and HSC transplant.

Results (Mouse)

The integrated model was summarized in the Fig 2(A-C). The arrows in Fig 2A represented direction of cell differentiation, proliferation, trafficking, and death. The long-term hematopoietic stem cells (LT-HSC) were capable of self-renewal and could differentiate to short-term hematopoietic stem cells (ST-HSC). ST-HSC could differentiate to multipotent progenitor cells (MPP). MPP could differentiate to common myeloid progenitor (CMP) and common lymphoid progenitor (CLP). CMP could differentiate to burst forming unit-erythroid (BFU-E) and granulocyte-monocyte progenitors (GMP). BFU-E could further differentiate to colony forming unit-erythroid (CFU-E), then reticulocytes (RET) and red blood cells (RBC). Hemoglobin (Hb) were synthesized in RETs and RBCs. The concentration of Hb in blood determined the oxygen level in blood, and subsequently imposed a negative feedback on CFU-E amplification. The erythrocytes differentiation submodel (Fig 2A) was scaled from humen to mice by reparameterizing mean residence time and amplification number using physiologically informed values. CLP was added to link the HSC differentiation with B cell and T cell development. GMP and the granulocytes (GM) differentiation were added to the models.

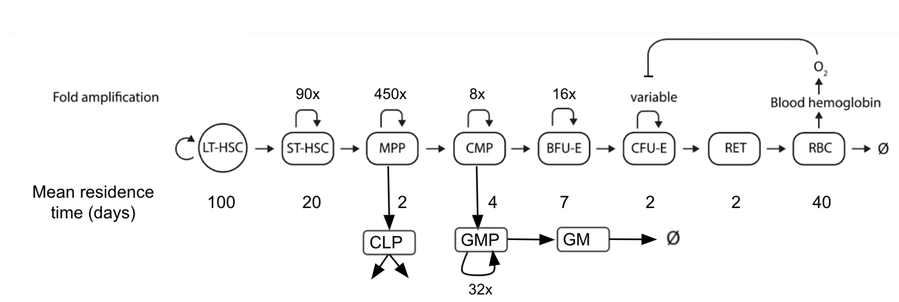

Fig 2A. Mouse HSC differentiation diagram on erythroid arm and other progenitor in bone marrow.

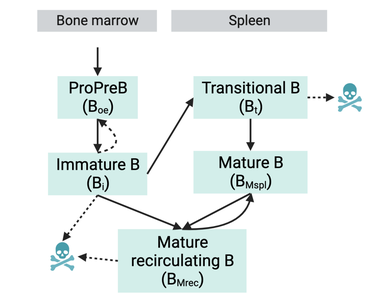

Fig 2B. B cell development.

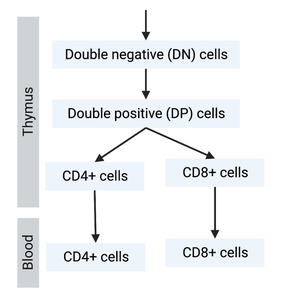

Fig 2C. T cell development in thymus.

The mouse model was parameterized based on literature, and could predict steady state (**Table 1**) and the reconstitution of RBC, B cells, and T cells after HSC transplant (**Fig 3**).

Table 1. Predicted vs observed mouse cell count and Hb concentration.

Cell type	Predicted	Observed
MPP	60k	75k-92k
CMP	2M	755k- 3M
GMP	757k	1M
GM	8.4k/uL	1.95-12.01k/uL
RET	498k/uL	200 - 500k/uL
RBC	9.9M/uL	10.2M/uL
blood Hb	13.2g/dL	13.6 - 16.4g/dL
Hb in RBC	261g/L	270-330g/L
lymphocyte	1.8k/uL	0.12 - 24k/uL

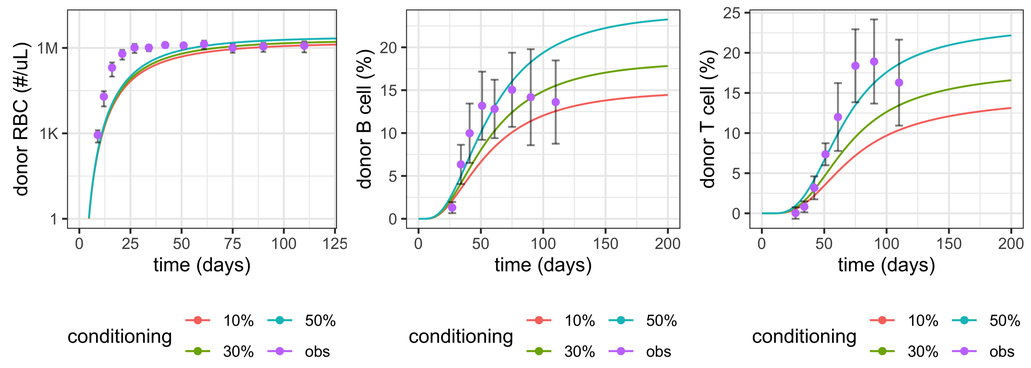

Fig 3. Predicted mouse RBC, B cell, and T cell reconstitution after HSC transplant (data obtained from [5]).

Results (Human)

The mouse model was scaled to human based on physiology. Especially, the scaling of bone marrow B cell capacity was based on cellularity. Naive T cell dynamics in lymph nodes (LN) and peripheral tissues [4] were also incorporated to capture the different mechanism for naive T cell maintenance (Fig 4B): in mice, thymic output is the main source of ;naive T cell in humans, naive T cell proliferation in peripheral tissue and blood has a prominent role [6,7].

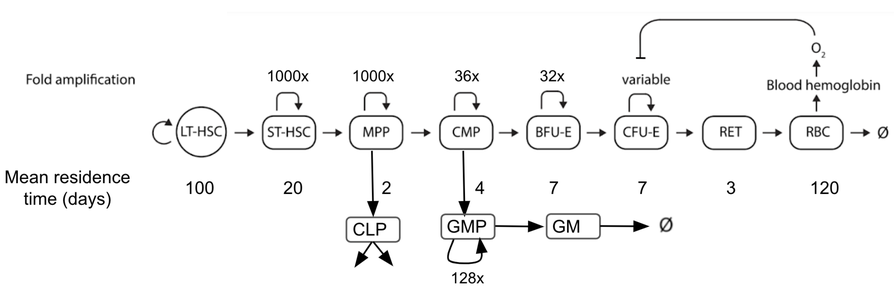

Fig 4A. Human HSC differentiation diagram on erythroid arm and other progenitor in bone marrow.

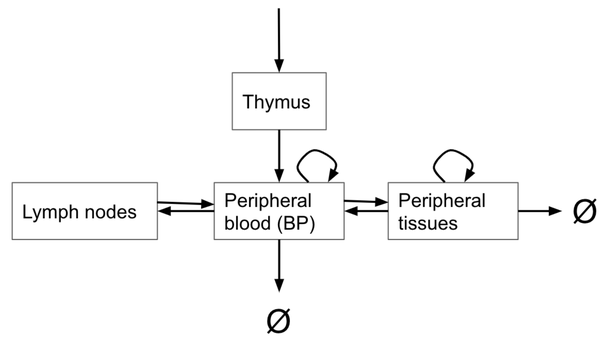

Fig 4B. Human naive T cell maintenance diagram.

Table 2. Predicted vs observed human cell count.

Cell type	Predicted	Observed
RBC (/uL)	3.9M	4M
Hb (g/dL)	13.2	12-15
thymic output (/day)	32M	10M-2700M
granulocyte (/uL)	1.2k	1k-8k
T cell (heathy) (/ul)	662	1243
T cell (ADA-SCID) (/ul)	149	138
B cell (healthy) (/uL)	137	101
B cell (ADA-SCID) (/uL)	61	0

The integrated human model recapitulated cell count in healthy humans and patients with ADA-SCID (**Table 2**). The death rates for DP cells (in thymuses) and splenic mature B cells were adjusted to account for ADA-SCID [8].

The integrated model recapitulated blood cell and hemoglobin reconstitution after gene therapy in those with sickle cell disease (SCD) (**Fig 5**). The model captured the lowering of RET count up to 6 months after the gene therapy, as well as the increase of HbA^{T87Q}, a Hb that only existed in transduced cells.

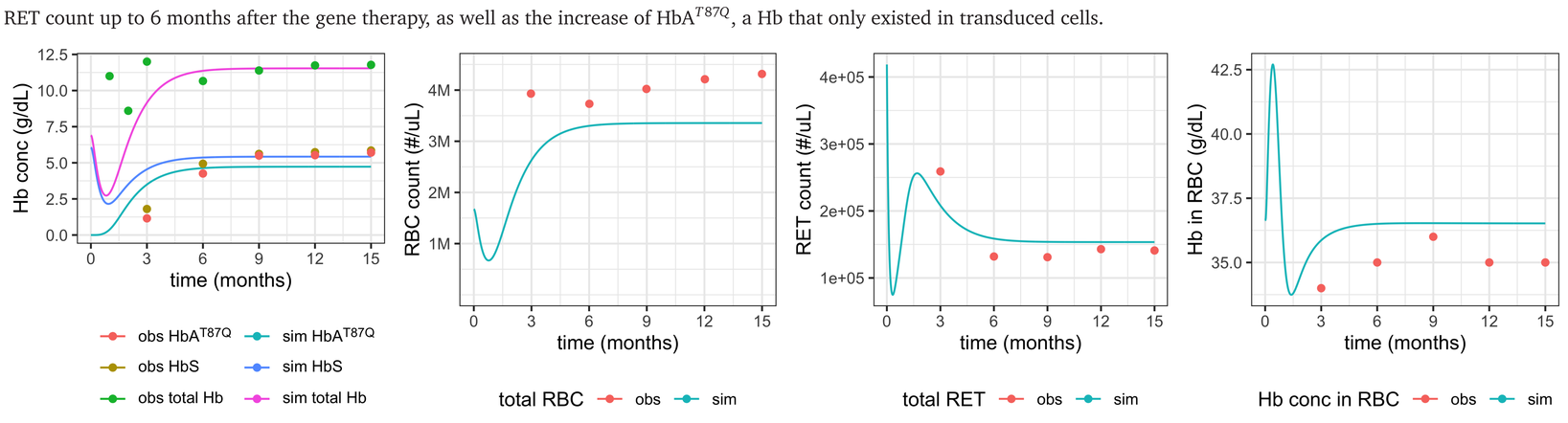

Fig 5. Predicted Hb, RBC, RET reconstitution in a SCD patient (data obtained from [9]).

The integrated model recapitulated immune cell reconstitution after gene therapy in those with ADA-SCID (**Fig 6**). Note the total amount of CD34+ cells infused into this patient was estimated based on the patient's age and sex (seven-month-old female). Reconstitution of GM matched less well compared to B cells and T cells, suggesting myeloid arm of this model could be further developed.

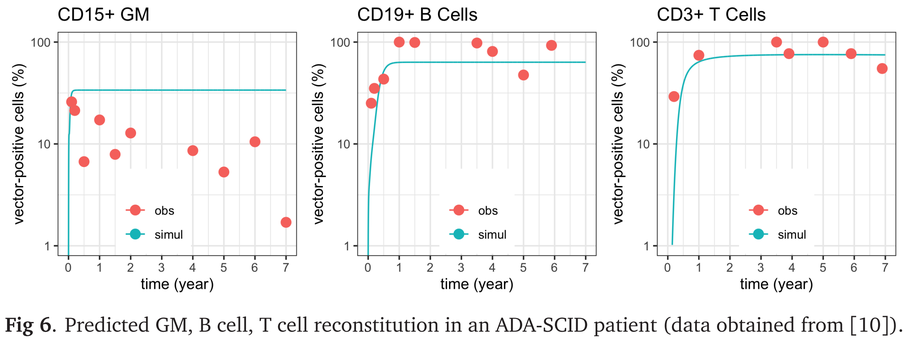

Fig 6. Predicted GM, B cell, T cell reconstitution in an ADA-SCID patient (data obtained from [10]).